J. Am. Soc. Mass Spectrom. (2012) 23:935–941
DOI: 10.1007/s13361-012-0355-5

RESEARCH ARTICLE

Laser-Induced Thermal Desorption Facilitates Postsource Decay of Peptide Ions

Shin Hye Kim,[1,2] Aera Lee,[1] Jae Yong Song,[3] Sang Yun Han[1]

[1]Center for Nano-Bio Convergence, Korea Research Institute of Standards and Science, Daejeon, Republic of Korea
[2]Department of Chemistry, Chungnam National University, Daejeon, Republic of Korea
[3]Center for Nanocharaterization, Korea Research Institute of Standards and Science, Daejeon, Republic of Korea

Abstract

We investigated the thermal mechanism involved in laser desorption/ionization (LDI) of thermally labile molecules from the flat surfaces of amorphous Si (a-Si) and crystalline Si (c-Si). a-Si was selected for this study because of its thermal property, such as low thermal conductivity; thus, it was predicted to be highly susceptible to laser-induced surface heating. By virtue of lack of surface nanostructures, the flat surfaces offer a simple model system to focus on the thermal mechanism, avoiding other effects, including possible non-thermal contributions that can arise from the physical existence of surface nanostructures. For the energetics study, the internal energies of substituted benzylpyridinium ions produced by LDI on the bare and coated surfaces of a-Si and c-Si were obtained using the survival yield method. The results, including LDI thresholds, ion yields, and internal energies all suggested that the LDI mechanism would be indeed thermal, which is most likely promoted by thermal desorption caused by laser-induced surface heating. In addition, the LDI process driven by laser-induced thermal desorption (LITD) was also found to be capable of depositing an excessive internal energy in resulting LDI ions, which underwent a dissociation. It exhibited the essentially same features as in postsource decay (PSD) in MALDI-TOF/TOF mass spectrometry. We report that the LDI process by LITD offers not only a way of intact ionization but also a facile means for PSD of peptide ions, which this work demonstrates is well suited to peptide sequencing using TOF/TOF mass spectrometry.

Key words: Laser desorption/ionization (LDI), Laser-induced thermal desorption (LITD), Postsource decay (PSD), Internal energy

Introduction

Laser desorption/ionization (LDI) of intact biomolecules from surfaces has been a subject of extensive studies in recent years [1]. By avoiding the use of matrixes, LDI provides a way around shortcomings from matrixes that are inevitably employed in MALDI mass spectrometry. In addition, the phenomenon of direct LDI of thermally labile molecules from surfaces is intriguing itself and worth a study, where the fundamental interaction of surfaces with photon and analytes is deeply involved.

In pursuit of LDI methods that can be alternatives to the conventional MALDI method, LDI on various nanostructured surfaces have been investigated. The LDI process of thermally labile molecules was first found to occur on the nanoporous surfaces of crystalline Si (c-Si) formed by photo-electrochemical etching [1, 2]. Without the surface porosity of a sub-micrometer dimension on c-Si, the LDI process was hardly observed to take place. Later on, the surfaces of c-Si tailored with various nanostructures were also demonstrated for their capabilities for efficient LDI, the examples of which include

Electronic supplementary material The online version of this article (doi:10.1007/s13361-012-0355-5) contains supplementary material, which is available to authorized users.

Correspondence to: Sang Yun Han; *e-mail:* sanghan@kriss.re.kr

Received: 31 October 2011
Revised: 27 January 2012
Accepted: 30 January 2012
Published online: 23 February 2012

porous Si surfaces formed by various methods [3], Si nanowires [4, 5], clathrate-structured Si surfaces [6], Si microcolumn and nanoposts arrays [7, 8], as well as commercial sample plates such as NALDI (Bruker-Daltonics, Bremen, Germany) [9]. Accordingly, the utilization of surface nanostructures has been common and in fact considered to be indispensable in the previous developments of high-efficiency LDI surfaces.

Due to the complex nature of LDI process, understanding of the detailed LDI mechanism still requires a further study. However, previous studies recognized the possible role of laser-induced surface heating, which has provided a reasonable account for energy transfer enabling intact desorption of molecules from nanostructured surfaces [3, 10, 11]. In the thermal mechanism, the surface nanostructures provide a thermal conduction barrier that tends to trap absorbed laser energy momentarily in the nano-dimension. It thus causes a rapid surface heating, which may promote intact desorption of thermally labile molecules [12, 13]. On the other hand, non-thermal contributions to the desorption process have also been proposed. For example, the bottleneck effect in energy transfer, when combined with shockwaves created by the physical existence of nanostructures, was discussed to assist the LDI process [14]. Due to the coexistence of various thermal and non-thermal components in the nanostructure-assisted LDI process, the investigation of the LDI mechanism on nanostructured surfaces has had to be complicated.

Although not plenty, a few reports are known for LDI of thermally labile molecules from flat surfaces (i.e., surfaces without surface nanostructures). The examples include the flat surfaces of amorphous Si (a-Si) [3] and commercially available Al foils [15]. In particular, LDI of peptides pronounced on the flat a-Si surfaces is notable because, as found in the previous studies, LDI of thermally labile molecules from the flat surfaces of c-Si has never been known before [1, 2]. In fact, the room-temperature optical and thermal properties of a-Si are comparable to those of c-Si, except a discernable difference in thermal conductivity. The different LDI behaviors, thus, can be suggested to be due to the difference in thermal conductivity between the two phases of Si, which is most likely related to laser-induced surface heating. In addition, the lack of surface nanostructures also offers a unique opportunity to focus on the thermal desorption involved in the LDI process [16, 17], which otherwise would be complicated with other effects arising from surface nanostructures. It includes the dependence of LDI efficiency on structural parameters such as aspect ratios [10], and possible non-thermal contributions such as shockwaves that can be blended in the thermal mechanism [14].

In recent years, the investigation of nanostructured surfaces for LDI mass spectrometry has not been solely limited to the subject of soft ionization. It attempts to extend its scope toward the functional LDI surfaces that further allow the characterization of analytes, providing such capabilities as in-source decay (ISD) and postsource decay (PSD) [9, 18]. However, both fragmentation techniques without the aid of surface nanostructures have not been known yet.

In this paper, we explored the thermal mechanism, more specifically, laser-induced thermal desorption (LITD) [16, 17], involved in the LDI process using the flat surfaces of a-Si and c-Si. In an effort to characterize the LITD process, we diagnosed the internal energies of substituted benzylpyridinium (BP) ions produced by pulsed laser irradiation from the flat surfaces using the survival yield method [19, 20]. As a result, we demonstrate in this study that LITD is not only a way for direct LDI of thermally labile molecules, but it also can provide a facile way to increase the internal energy of intact LDI ions, leading to PSD of peptide ions suitable for peptide sequencing using modern TOF/TOF mass spectrometry.

Materials and Methods

Clonidine (monoisotopic mass: 229.0 Da), azithromycin (749.0 Da), bradykinin 1-5 (572.7 Da), bradykinin 1-7 (756.9 Da), angiotensin II (1046.2 Da), Substance P (1347.6 Da), and somatostatin (1637.9 Da) were purchased from Sigma-Aldrich (Suwon, Korea). Octadecyltrichlorosilane (OTS; $CH_3(CH_2)_{17}SiCl_3$) was obtained from Sigma-Aldrich and undecyltrichlorosilane (UTCS; $CH_3(CH_2)_{10}SiCl_3$) was from Gelest, Inc. (Morrisville, PA). HPLC-grade methanol, hexane, and isopropyl alcohol (IPA) were from Merck (Seoul, Korea). Other high-purity reagents, including acetonitrile (ACN), methylene chloride, and CHCA (α-cyano-4-hydroxycinnamic acid) were purchased also from Sigma-Aldrich. Substituted BP preformed ions, 4-methoxy-BP, 4-methly-BP, and 4-chloro-BP were custom-synthesized by Hanchem Co. (Daejeon, Korea). The reagents were used without further purification.

Preparation of a-Si Surface and Surface Coating with Silane Compounds

The a-Si surfaces were prepared in-house. A Si target was sputtered with a 1 keV DC Ar ion beam and deposited on a rotating Si wafer (6 in. diameter, boron-doped, 1-10 ohm-cm; LG Siltron Inc., Kumi, Korea) at room temperature. The Si wafer was also used to provide the flat surfaces of c-Si in this study. The thickness of a-Si layer was prepared to be 100 nm. The root-mean-square surface roughnesses measured by atomic force microscopy (AFM; XE-150, PSIA, Suwon, Korea) were 0.14 and 0.07 nm for the surfaces of prepared a-Si and c-Si wafer, respectively.

The surfaces of a-Si and c-Si were further coated using OTS and UTCS [5]. The chips were first cleaned by sonication in 100% IPA for 30 s, washed in deionized water (Milli-Q; Millipore Korea, Seoul, Korea), and then dried under a gentle flow of nitrogen. After the cleaning step, the chip surfaces were further cleaned using a super-piranha solution (H_2O_2, HNO_3, and H_2SO_4 in a 10:1:6 volume ratio). Immediately after the piranha treatment, surface derivatization was carried out by dipping the cleaned chips in the silane solution (1 mM in hexane) in a nitrogen glove box for 16 h. The chips were cleaned using methylene

chloride and IPA and dried in a nitrogen gas flow, and stored in a vacuum dessiccator until the experiments.

LDI Mass Spectrometry

In this work, a MALDI-TOF/TOF mass spectrometer (Autoflex III; Bruker-Daltonics, Leipzig, Germany) was used, which was equipped with a 355 nm pulsed laser operated at 200 Hz. The full width at half maximum (FWHM) of a laser pulse was measured to be 7 ns using a high-speed photodiode. The maximum pulse energy was 5 μJ when measured at the sample position, and the laser beam diameter was set to be about 100 μm. The parameters give an estimate of 9×10^6 Wcm^{-2} for the laser irradiance (I), when the laser energy is 4.5 μJ/pulse (90%). The laser power is reported in this work as a relative laser power, that is, the percentage power (%) relative to the maximum value of 5 μJ, which was obtained from the setting values in the control program (flexControl; Bruker-Daltonics, Bremen, Germany). Typically, a laser power of 75%–80% was used to take a LDI mass spectrum, and a power of 90% or higher was used to create PSD of peptide ions. In the PSD experiments, the LIFT-TOF/TOF method adapted by the commercial instrument was utilized [21]. For MALDI experiments, CHCA was used as matrix (5 mg/mL in 50% ACN including 0.5% TFA).

Determination of Internal Energy of BP Ions

To interrogate the internal energy of LDI ions, we employed the survival yield method using a series of substituted benzylpyridinium (BP) ions. In this study, three BP ions (R-Bz-Py^+) with a different substituent (R) on the benzyl group, 4-methoxy-BP (E_c=1.3 eV), 4-methly-BP (1.6 eV), and 4-chloro-BP (1.73 eV), were employed, covering a range of critical energies (E_c) for the unimolecular decomposition reaction (Figure 1).

The survival yield method for MALDI was discussed in-depth in a previous paper [20], the method and assumptions

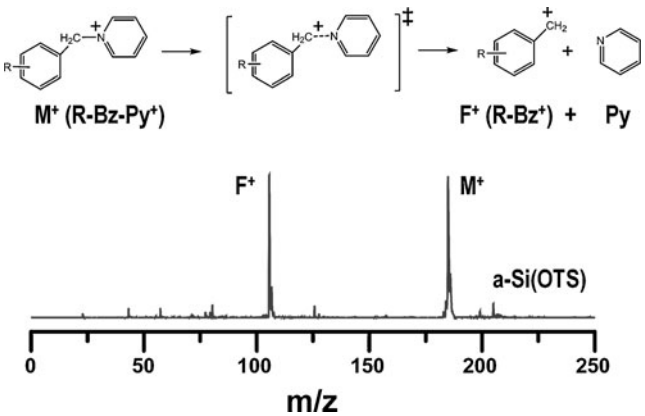

Figure 1. Schematic of the dissociation reaction of substituted BP ions in the survival yield method and the resulting mass spectrum for 4-methly-BP (2 pmol) obtained from a-Si (OTS) in linear TOF mode

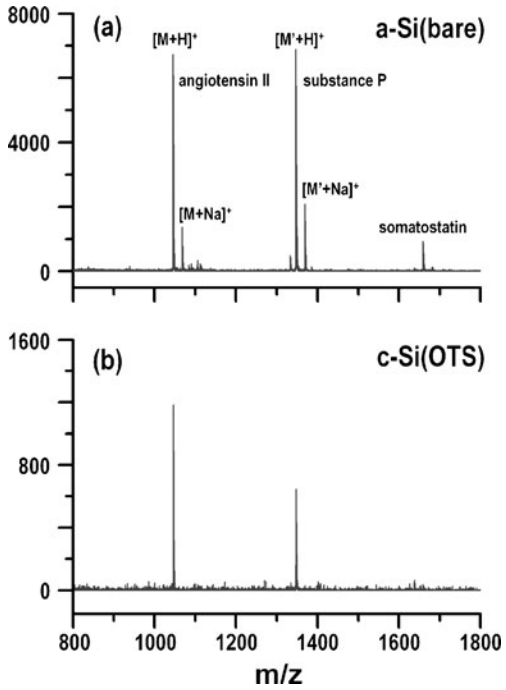

Figure 2. LDI mass spectra of a peptide mixture of angiotensin II, Substance P, and somatostatin obtained from **(a)** a-Si(bare) (2 pmol, 88% laser power) and **(b)** c-Si(OTS) surfaces (5 pmol, 92% laser power)

of which was directly adapted by this work. Briefly, the dissociation of parent BP ions, M^+ (R-Bz-Py^+), to the substituted benzyl cation fragment, F^+ (R-Bz^+), was monitored as a function of laser power using a TOF mass spectrometer in linear mode. The survival yield (SY) of BP ions was then obtained by $I(M^+)/[I(M^+) + I(F^+)]$, where $I(M^+)$ and $I(F^+)$ are the abundances of the parent ion and the fragment ion, respectively. The observed survival yield gave an experimental rate constant (k_{exp}) for the unimolecular decomposition by $k_{exp}=-(1/\tau)\ \ln(SY)$, where 100 ns was used for the characteristic reaction time (τ) for all BP ions. These experimental rate constants were further compared with the

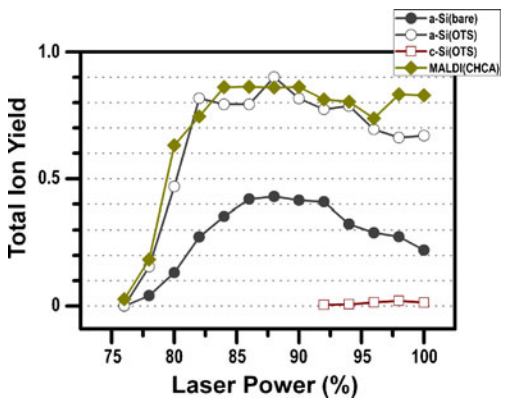

Figure 3. Plots of total ion yields for 4-methoxy-BP, $[I(M^+) + I(F^+)]$, produced by LDI on a-Si(bare) filled circle (●), a-Si(OTS) open circle (○), and c-Si(OTS) open square (□) surfaces, and by MALDI using CHCA matrix filled diamond (♦)

values predicted by RRKM (Rice-Ramsperger-Kassel-Marcus) theory, yielding the estimates for the internal energy of BP ions produced in the gas phase by the LDI process.

Results and Discussion

Laser-Induced Surface Heating of Flat Si Surfaces

In an effort to look into the thermal mechanism more closely, we carried out a comparative study on LDI using the flat surfaces of a-Si and c-Si. The bulk thermal property of a-Si is very close to that of c-Si, except a noticeable difference in thermal conductivity (K). The thermal conductivity of a-Si (5.5 Wm^{-1} K^{-1}) is much lower than that of c-Si (150 Wm^{-1} K^{-1}) [22, 23], which can play a role in preventing the absorbed laser energy from being quickly dispersed into the bulk by heat conduction. Using 1.65 Jcm^{-3} K^{-1} for the specific heat (C_p) of a-Si, one can obtain an estimate of about 90 nm for the depth of conductive heating ($D = [Kt/C_p\pi]^{1/2}$) after a laser irradiation for a characteristic time (t=7 ns) [11]. As for c-Si, its thermal properties (K=150 Wm^{-1} K^{-1} and C_p=1.67 Jcm^{-3} K^{-1}) give a much longer depth (D) of about 450 nm. The low thermal conductivity of a-Si can drastically increase the surface temperature upon absorption of pulsed laser energy. In this regard, the low thermal conductivity is in fact the property that is analogous to the physical conduction barriers presented by surface nanostructures, which enhance laser-induced surface heating.

Using the literature values (K and C_p) along with a model laser pulse in triangular shape with 7 ns at FWHM, the increase in surface temperature because of the absorption of a laser pulse can be simulated using the analytical solutions for the heat

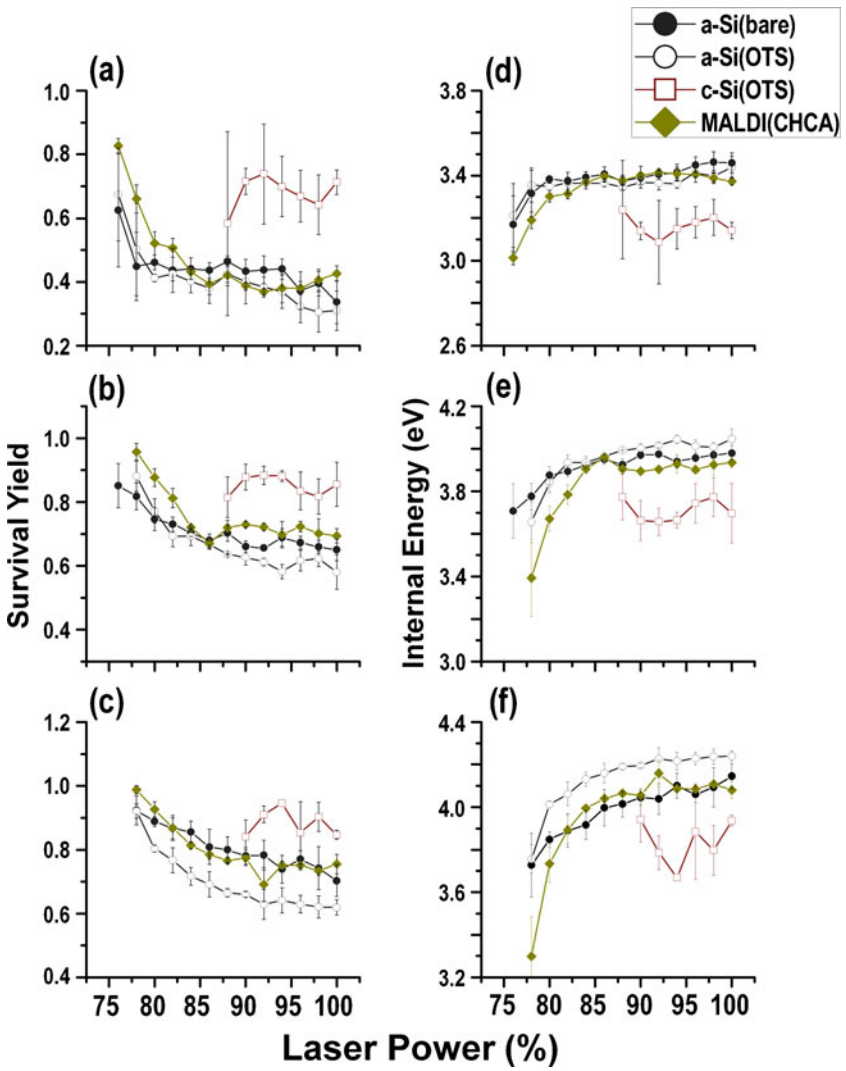

Figure 4. Plots of survival yields for **(a)** 4-methoxy-BP (E_c=1.3 eV), **(b)** 4-methyl-BP (1.6 eV), and **(c)** 4-chloro-BP (1.73 eV), along with the corresponding internal energies for **(d)** 4-methoxy-BP, **(e)** 4-methyl-BP, and **(f)** 4-chloro-BP (2 pmol). The results were obtained from a-Si(bare) filled circle (●), a-Si(OTS) open circle (○), and c-Si(OTS) open square (□) surfaces, and using MALDI (CHCA) filled diamond (♦), as a function of laser power. The error bar indicates the standard deviation evaluated from three independent measurements

diffusion equation [16]. The simulation shows that the absorption of laser energy rapidly increases the surface temperature reaching to the peak temperature at around 9 ns. It also predicts that the peak temperatures achievable on a-Si and c-Si surfaces are quite different. For example, the increase in surface temperature as high as 1400 K was predicted for a-Si, whereas only 300 K was calculated for c-Si, when a laser pulse of 6 MW/cm^2 was assumed to be fully absorbed by the surfaces (see Supplemental Information). Although solving the equation using the room temperature thermal properties may have limitations in predicting the peak surface temperature created in such a short time duration (<20 ns) in the high temperature region, the results still indicate that the difference in the thermal conductivity of a-Si and c-Si can create a substantial difference in laser-induced surface heating.

LDI of Thermally Labile Molecules from Flat Si Surfaces

We started with examining LDI of molecules from the bare surfaces of a-Si, a-Si(bare). A set of test molecules was used, which included small drug molecules (clonidine and azithromycin), and peptides (bradykinin 1-5, bradykinin 1-7, angiotensin II, Substance P, and somatostatin), representing a range of molecular weights up to 1600 Da. When the flat surfaces of a-Si, a-Si(bare), were used for LDI experiments, all of the test molecules led to the formation of intact protonated molecules (data not shown), as reported by a previous study [3]. In contrast, LDI from a clean c-Si surface (Si wafer) did not produce any of intact ions except for a trace amount of clonidine ions.

On the other hand, we also examined the effect of surface derivatization. We employed the surface coating with OTS [5]. The surface derivatization was found to enhance the LDI efficiency on the coated a-Si surfaces, a-Si(OTS), for a factor of two to several against the test molecules. The detection limit for a-Si(OTS) was measured to be better than 0.05 and 10 fmol for clonidine and angiotensin II, respectively. Interestingly, even the OTS-coated c-Si surfaces, c-Si(OTS), began to exhibit a LDI activity. The efficiency on c-Si(OTS) was still very low so that a high level of laser power (>90%) and sample load (>5 pmol) was necessary to observe the intact ions of peptides (Figure 2).

In this work, we employed the OTS-coated flat surfaces of a-Si and c-Si because both surfaces have the same chemical property because of the same passivation layer (OTS) and exhibit the LDI activity for thermally-labile molecules such as peptides as well.

Internal Energy of BP Ions Produced by LDI on Flat Si Surfaces

In order to characterize the LITD process, we determined the internal energy of BP ions produced from a-Si(OTS) and c-Si(OTS). The use of preformed ions, which does not require the charge-acquiring step for the LDI process, allowed this study to focus more on the desorption process. In the study, we chose the average internal energy instead of the energy distribution [20].

Figure 3 shows the plots of total ion yields for 4-methoxy-BP, [I(M^+) + I(F^+)], displaying the LDI efficiencies for the different surfaces of a-Si(bare), a-Si(OTS), and c-Si(OTS). For comparison, the results for MALDI using CHCA matrix, MALDI(CHCA), are also given. As shown in the results, a-Si (OTS) and MALDI(CHCA) were found to possess similar near-threshold behaviors and comparable LDI efficiencies. a-Si (bare) surfaces also exhibited a similar laser power threshold. However, its LDI efficiency was lower than those of a-Si(OTS) and MALDI(CHCA). On the other hand, LDI from c-Si(OTS), even after the surface coating with OTS, was still inefficient, exhibiting a high threshold (>90%) and very low ion yields.

The survival yields and obtained internal energies of three BP ions produced from a-Si(bare), a-Si(OTS), and c-Si(OTS) are given in Figure 4, along with the results for MALDI (CHCA). The results display some characteristic features for the LDI process. First, LDI on c-Si(OTS) requires a higher laser power than on a-Si(OTS). It is in good agreement with the fact that a-Si is more susceptible to laser-induced surface heating than c-Si because of its low thermal conductivity. Second, at a given high laser power, such as 95%, the internal energy of ions

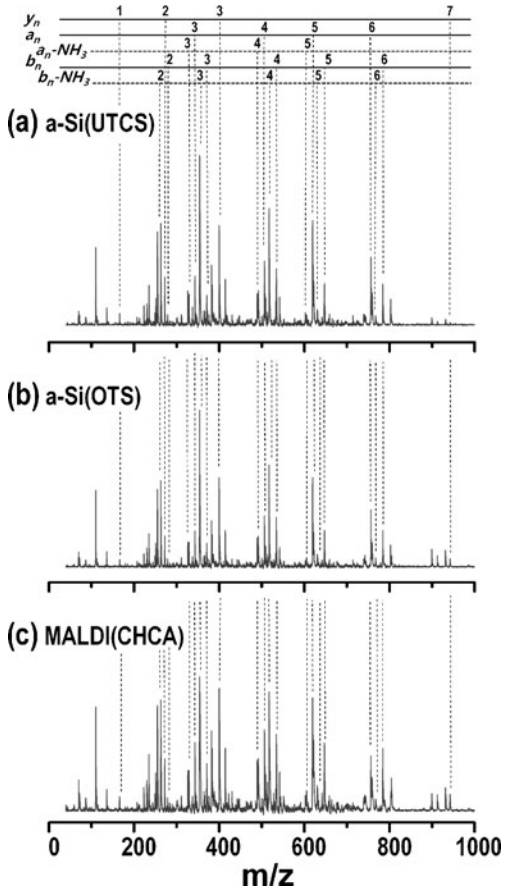

Figure 5. PSD spectra of angiotensin II obtained from **(a)** a-Si(UTCS), **(b)** a-Si(OTS) surfaces, and **(c)** using MALDI (CHCA); (2 pmol, 95% laser power, 400 shots)

produced on a-Si(OTS) is about 0.4 eV higher than that produced from c-Si(OTS). The higher internal energy for a-Si (OTS) supports that laser-induced surface heating is indeed deeply involved in the LDI mechanism. Third, in comparison between a-Si(bare) and a-Si(OTS), the internal energies of both cases appear to be comparable, despite the different LDI efficiencies (Figure 3). It suggests that the main driving force for the LDI process relies on the substrate property rather than the surface property due to coatings.

More importantly, the internal energy as a function of laser power increases in the above-threshold region (75%~85%), which is noticeable compared with the previous results on nanostructured surfaces. Previously, little change was found in the internal energies of BP ions produced from porous Si and Si nanoposts, and was interpreted to be due to the contribution of non-thermal effects [24]. The observed increase thus suggests that such nonthermal effects may not be involved in this study. Accordingly, the features revealed by the internal energy study indicate that the LDI process from the flat Si surfaces is indeed mainly driven by a thermal mechanism; more specifically, the LITD process caused by laser-induced surface heating, although the ionization step (i.e., the charge-acquiring process) is still a subject of further study.

PSD of Peptide Ions Produced by LDI on Flat Si Surfaces

The MALDI method using CHCA matrix is a common choice for PSD-TOF/TOF mass spectrometry, where the method induces the extensive fragmentation of peptide ions under high MALDI laser fluences. The resulting fragment ions provide the sequence information for the peptides [25].

As shown in Figure 4, near the threshold MALDI(CHCA) apparently produces colder ions (i.e., ions with a lower internal energy). However, the internal energy of MALDI ions increases rapidly with the increased laser power and becomes comparable to that of LDI ions from a-Si(OTS) in the high laser power regime (>90%), which is in fact the high energy regime where MALDI(CHCA) creates PSD of peptide ions. This result suggests a new usage of the LITD process as a way of supplying the excessive internal energy necessary to cause PSD for peptide characterization without employing matrixes.

In order to corroborate such a postulation, we carried out TOF/TOF mass spectrometry of peptide ions [21], angiotensin II and Substance P, produced by LDI on a-Si(OTS) and a-Si (UTCS) (Figure 5, see also Supplemental Information). Indeed, all TOF/TOF spectra obtained from LDI on the flat a-Si surfaces in the high laser power regime (>90%) clearly showed pronounced PSD of the peptide ions. The PSD spectra exhibited the essentially same backbone cleavages as generated in MALDI(CHCA) with a similar intensity pattern. The essentially same results indicate that their decay mechanisms are identical and are caused by the excess internal energy, although they resulted from the different ionization methods.

Conclusion

In this study, we investigated the LDI process occurring on the flat surfaces of a-Si and c-Si. In a comparative study on the internal energy of BP ions from the two Si surfaces, the LDI mechanism from the flat Si surfaces was revealed to be largely thermal, governed by LITD caused by laser-induced surface heating. In addition, LITD was also found to be capable of depositing an excessive internal energy in LDI ions in the high laser power regime, which could lead to a metastable decomposition of peptide ions. In conclusion, the matrix-free LDI method driven by the thermal mechanism is not only a way of intact ionization of thermally labile molecules. We report that it also presents a facile means to cause PSD of peptide ions suitable for TOF/TOF mass spectrometry, by demonstrating pronounced PSD of peptide LDI ions, which is comparable to the MALDI(CHCA) case, for the first time, from the flat surfaces that are amenable to laser-induced surface heating.

Acknowledgments

The authors acknowledge support for this research from the Converging Research Center Program through the NRF, funded by MEST (2011 K000887). This work was also supported by the Biosignal Analysis Technology Innovation Program (2011-0027718) of MEST via KOSEF.

References

1. Peterson, D.S.: Matrix-free methods for laser desorption/ionization mass spectrometry. *Mass Spectrom. Rev.* **26**, 19–34 (2007)
2. Wei, J., Buriak, J.M., Siuzdak, G.: Desorption/ionization mass spectrometry on porous silicon. *Nature* **399**, 243–246 (1999)
3. Alimpiev, S.; Grechnikov, A.; Sunner, J.; Karavanskii, V.; Simanovsky, Ya.; Zhabin, S.; Nikiforov, S. On the role of defects and surface chemistry for surface-assisted laser desorption ionization from silicon. *J. Chem. Phy.* **128**, 014711 (2008)
4. Go, E.P., Apon, J.V., Luo, G., Saghatelian, A., Daniels, R.H., Sahi, V., Dubrow, R., Cravatt, B.F., Vertes, A., Siuzdak, G.: Desorption/ionization on silicon nanowires. *Anal. Chem.* **77**, 1641–1646 (2005)
5. Piret, G., Drobecq, H., Coffinier, Y., Melnyk, O., Boukherroub, R.: Matrix-free laser desorption/ionization mass spectrometry on silicon nanowire arrays prepared by chemical etching of crystalline silicon. *Langmuir* **26**, 1354–1361 (2010)
6. Northen, T.R., Yanes, O., Northen, M.T., Marrinucci, D., Uritboonthai, W., Apon, J., Golledge, S.L., Nordstrom, A., Siuzdak, G.: Clathrate nanostructures for mass spectrometry. *Nature* **449**, 1033–1036 (2007)
7. Walker, B.N., Razunguzwa, T., Powell, M., Knochenmuss, R., Vertes, A.: Nanophotonic ion production from silicon microcolumn arrays. *Angew. Chem. Int. Ed.* **48**, 1669–1672 (2009)
8. Walker, B.N., Stolee, J.A., Pickel, D.L., Retterer, S.T., Vertes, A.: Tailored silicon nanopost arrays for resonant nanophotonic ion production. *J. Phys. Chem. C* **114**, 4835–4840 (2010)
9. Guénin, E., Lecouvey, M., Hardouin, J.: Could a nano-assisted laser desorption/ionization target improve the study of small organic molecules by laser desorption/ionization time-of-flight mass spectrometry? *Rapid Commun. Mass Spectrom.* **23**, 1395–1400 (2009)
10. Shin, W.J., Shin, J.H., Song, J.Y., Han, S.Y.: Effects of ZnO nanowire length on surface-assisted laser desorption/ionization of small molecules. *J. Am. Soc. Mass Spectrom.* **21**, 989–992 (2010)
11. Alimpiev, S., Nikiforov, S., Karavanskii, V., Minton, T., Sunner, J.: On the mechanism of laser-induced desorption-ionization of organic compounds from etched silicon and carbon surfaces. *J. Chem. Phys.* **115**, 1891–1901 (2001)
12. Daves Jr., G.D.: Mass spectrometry of involatile and thermally unstable molecules. *Acc. Chem. Res.* **12**, 359–365 (1979)

13. Beuhler, R.J., Flanigan, E., Greene, L.J., Friedman, L.: Proton transfer mass spectrometry of peptides. A rapid heating technique for underivatized peptides containing arginine. *J. Am. Chem. Soc.* **96**(12), 3990–3999 (1974)
14. Luo, G., Chen, Y., Siuzdak, G., Vertes, A.: Surface modification and laser pulse length effects on internal energy transfer in DIOS. *J. Phys. Chem. B* **109**, 24450–24456 (2005)
15. Hsu, N.-Y., Tseng, S.Y., Wu, C.-Y., Ren, C.-T., Lee, Y.-C., Wong, C.-H., Chen, C.-H.: Desorption ionization of biomolecules on metals. *Anal. Chem.* **80**, 5203–5210 (2008)
16. Burgess Jr., D., Stair, P.C., Weitz, E.: Calculations of the surface temperature rise and desorption temperature in laser-induced thermal desorption. *J. Vac. Sci. Technol. A* **4**, 1362–1366 (1986)
17. Voumard, P., Zenobi, R.: Laser-induced thermal desorption of aniline from silica surfaces. *J. Chem. Phys.* **103**, 6795–6805 (1995)
18. Chen, Y., Vertes, A.: Adjustable fragmentation in laser desorption/ionization from laser-induced silicon microcolumn arrays. *Anal. Chem.* **78**, 5835–5844 (2006)
19. Collette, C., Drahos, L., Pauw, E.D., Vekey, K.: Comparison of the internal energy distributions of ions produced by different electrospray sources. *Rapid Commun. Mass Spectrom.* **12**, 1673–1678 (1998)
20. Luo, G., Marginean, I., Vertes, A.: Internal energy of ions generated by matrix-assisted laser desorption/ionization. *Anal. Chem.* **74**, 6185–6190 (2002)
21. Suckau, D., Resemann, A., Schuerenberg, M., Hufnagel, P., Franzen, J., Holle, A.: A novel MALDI LIFT-TOF/TOF mass spectrometer for proteomics. *Anal. Bioanal. Chem.* **376**, 952–965 (2003)
22. Volz, S., Feng, X., Fuentes, C., Guerin, P., Jaouen, M.: Thermal conductivity measurements of thin amorphous silicon films by scanning thermal microscopy. *Int. J. Thermophys.* **23**, 1645–1657 (2002)
23. Glazov, V.M., Pashinkin, A.S.: The thermophysical properties (heat capacity and thermal expansion) of single-crystal silicon. *High Temperature* **39**, 413–419 (2001)
24. Stolee, J.A., Chen, Y., Vertes, A.: High-energy fragmentation in nanophotonic ion production by laser-induced silicon microcolumn arrays. *J. Phys. Chem. C* **114**, 5574–5581 (2010)
25. Chaurand, P., Luetzenkirchen, F., Spengler, B.: Peptide and protein identification by matrix-assisted laser desorption ionization (MALDI) and MALDI-post-source decay time-of-flight mass spectrometry. *J. Am. Soc. Mass Spectrom.* **10**, 91–103 (1999)